

DOI: 10.1002/adem.200800162

# Propagation and Deflection of Shear Bands in Metallic Glass under Circumferential Constraint\*\*

By Jitang Fan, Zhefeng Zhang,\* Scott Xingyuan Mao and Jürgen Eckert

For monolithic bulk metallic glasses, deformation and fracture are always associated with the initiation and propagation of localized shear bands, finally leading to failure in a shear mode.<sup>[1,2]</sup> Thus, it is of considerable scientific interest to investigate the formation and propagation of shear bands in metallic glass experimentally and theoretically.<sup>[3-7]</sup> Generally, due to the long-range disorder and macroscopically isotropic nature of amorphous alloys,<sup>[8]</sup> shear bands often initiate along some shear plane, which is convenient to investigate the yielding or fracture criterion based on the observations of the angles between shear bands and stress axis.<sup>[9,10]</sup> For metallic glass composites, the primary shear bands are restrained due to the strong impeding effect of second phase particles or fibers, leading to the deflection or formation of secondary shear bands.<sup>[11-15]</sup> The same phenomenon also occurs in metallic glassy specimens with a small aspect ratio under compressive loading.<sup>[16,17]</sup> In addition, under bending or indentation, due to the complexity of the stress distribution, shear bands are not always planar but often proceed along some curved plane.<sup>[18-21]</sup> Especially, it is interesting to find that pro-

fuse shear bands appear on the surface of metallic glassy samples subjected to small punch test, forming completely symmetrical patterns with dense shear bands along both circumferential and radial directions, even for the highly brittle BMGs composites.<sup>[22]</sup>

The above findings illustrate that the formation and propagation of shear bands in metallic glass have a close relationship with the stress state and the circumferential limitation/constraint. This gives rise to an interesting question: how the stress condition and the circumferential limitation affect the initiation and propagation of shear bands? However, until now there are few reports with the explicit intent to investigate the propagation and deflection of shear bands by using a circumferential limiting boundary. In this letter, we introduce an unsymmetrical circumferential limiting boundary to a Zr-based metallic glass sample during the small punch test, in order to further reveal the propagation and deflection of shear bands. Finally, we propose a new strategy to enhance the plasticity by strengthening the surface of metallic glasses without any expenditure of the strength.

## Experimental

A  $Zr_{52.5}Cu_{17.9}Al_{10}Ni_{14.6}Ti_5$  master alloy was prepared by arc melting elemental Zr, Cu, Al, Ni, and Ti with a purity of 99.99% or better in a Ti-gettered argon atmosphere. The ingots were re-melted for several times, followed by casting into a copper molds with a cavity of  $3 \times 100$  mm. Analyzed by X-ray diffraction (XRD) using a Rigaku diffractometer with Cu-radiation as a source, the final sample shows only broad diffraction maxima without any peaks of crystalline phases, revealing the typical amorphous structure, in accord with the reference.<sup>[23]</sup> In the current study, the plastic deformation behaviors were investigated by means of the small punch test technique, which requires samples with 0.1 mm in thickness and 3 mm in diameter. The thin samples were sandwiched between the upper and lower dies, and then subjected to a load of 5 kg for 10 min, similar as the previous report.<sup>[22]</sup> For the present experiments, the upper guide hole was round and the lower was elliptical in order to introduce an asymmetric circumferential limiting boundary to the punched sample. In this case, the formed shear bands will distribute with an asymmetric pattern. After the small punch test, the samples were observed with a Quanta 600 scanning electron microscope (SEM) to reveal the propagation and deflection behaviors of the shear bands.

[\*] Dr. J. T. Fan, Prof. Z. F. Zhang  
Shenyang National Laboratory for Materials Science  
Institute of Metal Research  
Chinese Academy of Science  
Shenyang 110016, People's Republic of China  
E-mail: jtfan@imr.ac.cn, zhffzhang@imr.ac.cn  
Prof. S. X. Mao  
Department of Mechanical Engineering  
University of Pittsburgh  
Pittsburgh, PA 15261, USA  
Prof. J. Eckert  
IFW Dresden  
Institut für Komplexe Materialien  
Postfach 270116, D-01171 Dresden, Germany

[\*\*] The authors would like to thank the financially supporting by the National Natural Science Foundation of China (NSFC) under Grant No. 50401019, the "Hundred of Talents Project" by Chinese Academy of Science and the National Outstanding Young Investigator Grant for Z. F. Zhang under No. 50625103, 50871117 and 50890173.

Results and Discussions

Figure 1(a) shows SEM image of shear bands on the lower surface of metallic glass sample after the small punch test. Visibly, the distance from the center of the spherical indentation (shown by the dot) to the limiting boundary (shown by the dashed line) changes gradually. Due to the isotropic nature of metallic glass and the symmetrical stress or strain distribution around the center, many radiating shear bands firstly radiated from the center of spherical indentation and propagated with a proportional spacing (see Fig. 1(b)), just as the analysis in reference.<sup>[24]</sup> Meanwhile, there are many circumferential shear bands in different radius around the center of spherical indentation. In particular, the radial shear bands began to deflect near the end, due to the constraint imposed by the asymmetric limiting boundary (see Fig. 1(b)), which is similar to the report in reference.<sup>[11–21]</sup> Besides, the amplified image of Region A reveals that the deflection points are the demarcation points of radial shear bands (see Fig. 1(c)). The shear bands are thicker before the deflection point, and become weaker after the deflection point, indicated by the arrows. This illustrates that the limiting boundary prevents shear bands from growing into the cracks. More-

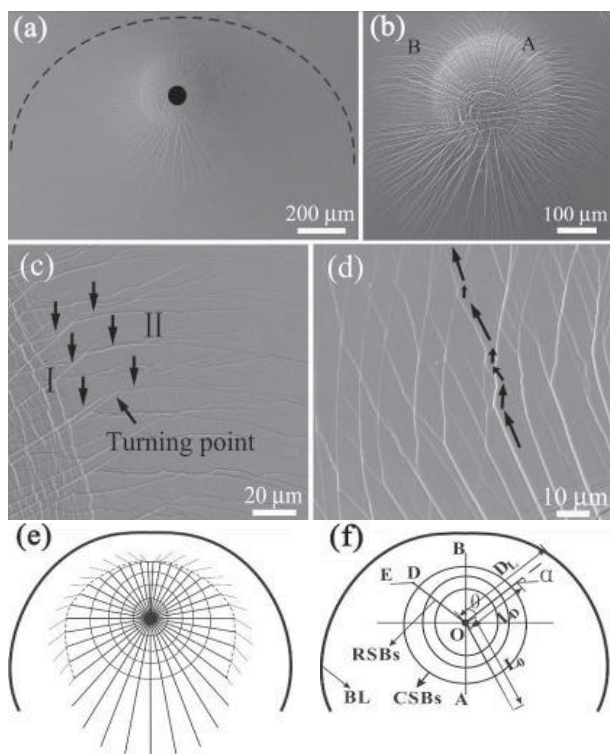


Fig. 1. (a) SEM image of shear bands on the lower surface of metallic glass specimen after small punch testing; (b) slightly magnified image designating the Regions A and B; (c,d) local amplified images of shear bands, corresponding to Regions A and B respectively; (e) illustration of the corresponding shear band morphology; (f) illustration of one typical shear band morphology. Here, RSBs denotes radial shear bands; CSBs denotes circumferential shear bands; D is the deflection point of shear band during propagation; O is the center of indentation;  $\theta$  is the rotation angle of the shear band relative to the vertical line;  $\alpha$  is the deflection angle of the shear band;  $L_D$  is the length of the shear band between center and deflection point;  $L_0$  is the intrinsic length of the shear band;  $L_T$  is the total length of the shear band, equal to  $OD+DE$ ;  $D_L$  is the distance from the center to the limiting boundary; BL is the limiting boundary.

over, at the tip of deflecting shear bands (see Region B in Fig. 1(b)), the shear bands interact with each other resulting in wriggling, implying the high plasticity,<sup>[25,26]</sup> marked by arrows in Figure 1(d).

From the SEM images, it is easy to find both the deflection angle and length of shear bands tend to change with the limiting boundary, illuminated in Figures 1(e,f). Thus, we carefully measured and accurately calculated the change of the following data:  $D_L, L_D, L_T, \alpha$  with the rotation angle,  $\theta$  shown in Figure 2. When the rotation angle,  $\theta$  increases, the distance,  $D_L$  will increase, depending on the experimental conditions. Accordingly, the length of shear bands between the center and deflection point,  $L_D$  and the total length of shear bands,  $L_T$  will increase too. However, the deflection angle,  $\alpha$  will decrease. This indicates that both the deflection point and deflection angle strongly depend on the distance,  $D_L$ . In other words, the prohibitive effect of the limiting boundary will decrease with the increase in the distance,  $D_L$ , which will be discussed in detail below.

At the position,  $\theta = 0^\circ$ , the distance,  $D_L$  is  $320 \mu\text{m}$ , which is the minimum under the current testing conditions, caused by the maximum impeding effect on the shear bands. In this case, the total length,  $L_T$  reaches its minimum value of  $260 \mu\text{m}$ , and the deflection angle,  $\alpha$  reaches its maximum value of  $42^\circ$ . With the increase in the distance,  $D_L$ , the impeding effect will decrease monotonically. For example, at the position,  $\theta = 130^\circ$ ,  $D_L$  reaches its maximum value of about  $920 \mu\text{m}$ , and the impeding effect seems to be negligible. The total length,  $L_T$  reaches its maximum value of about  $440 \mu\text{m}$ , and the deflection angle,  $\alpha$  decreases to the minimum of about  $5^\circ$ . Furthermore, at the position,  $\theta = 130 \sim 180^\circ$ , there is no limiting boundary to impede the propagation of shear bands, and the distance,  $D_L$  can be regarded as  $+\infty$ . Accordingly, the shear bands will not deflect, and the total length will remain nearly constant. Comparing the two positions at  $\theta = 130^\circ$  and  $\theta = 140^\circ$ , the total length,  $L_T$  largely increases from  $440 \mu\text{m}$  to  $475 \mu\text{m}$ , which provides strong evidence that the limiting boundary has a significantly prohibitive effect on the propagation of shear bands. The length,  $L_T$  reaches its maximum

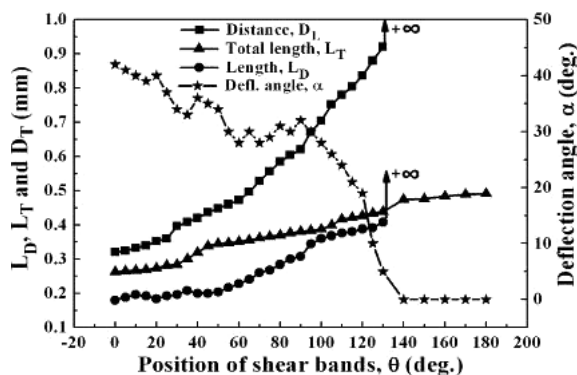


Fig. 2. Dependence of several critical parameters: the distance,  $D_L$ ; length of the shear bands between center and deflection point,  $L_D$ ; total length of the shear bands,  $L_T$ ; deflection angle,  $\alpha$ , on the rotation angle of shear bands relative to the vertical line,  $\theta$  at different positions (see Fig. 1(f)).

value of about 490  $\mu\text{m}$  under this loading condition at the position of  $\theta = 180^\circ$ , because no constraint would impede the propagation of shear bands. Accordingly, we define the maximum value as the intrinsic length  $L_0$  (here  $L_0 = 490 \mu\text{m}$ ) of shear bands under the current experimental conditions. According to the geometric relationship in Figure 1(f), the distance,  $D_L$  and the rotation angle,  $\theta$  follow the equation:

$$D_L = \sqrt{R^2 - D_0^2 \sin^2 \theta} - D_0 \cos \theta \quad (1)$$

Where,  $R$  is the radius of circumferential limiting boundary (here  $R = 750 \mu\text{m}$ ) and  $D_0$  is the deviation distance from the center of spherical indentation (shown by the dot) to the center of the limiting boundary (here  $D_0 = 400 \mu\text{m}$ ).

For quantitatively describing the restraining effect on the shear bands, we define a prohibitive ability,  $P_L$ , to evaluate the restraining degree of the limiting boundary, which can be expressed as:

$$P_L = (L_0 - L_D)/L_0 \quad (2)$$

Where,  $L_D$  is the length of shear band between the center and deflection point, and  $L_0$  is the intrinsic length of shear band, illustrated in Figure 1(f). Based on the experimental observations, we measured all the deflecting shear bands and plotted the dependence of the prohibitive ability,  $P_L$  on the distance,  $D_L$ . Notably, the prohibitive ability,  $P_L$  decreases with the increase in the distance,  $D_L$  (see Fig. 3(a)). By linear fitting, the following relation between them can be attained with an error range of  $\pm 0.02$ :

$$P_L(\%) = 0.92 - 0.86D_L \quad (3)$$

That vividly illustrates that the prohibitive ability,  $P_L$  decreases with the increase in the distance,  $D_L$ , with a sound inverse linear relationship. On the other hand, the deflection angles,  $a$  are quite different, depending on the position,  $\theta$  too. Therefore, another prohibitive ability,  $P_a$  was defined to characterize the deflection degree of shear bands, expressed by the following equation:

$$P_a(\%) = (a - 0)/a_{\max} = a/a_{\max} \quad (4)$$

Where,  $a_{\max}$  is the maximum deflection angle (here  $a_{\max} = 42^\circ$ ) of shear bands under the current experimental conditions. Clearly, Figure 3(b) shows that the prohibitive ability,  $P_a$  also follows an inverse linear relationship with the distance,  $D_L$ . The fitting equation is described as followed with an error range of  $\pm 0.03$ :

$$P_a(\%) = 1.22 - 0.92D_L \quad (5)$$

Besides, the total length of shear bands,  $L_T$  rises with the increase in the distance,  $D_L$ . Based on a number of statistic data, they approximately follow a linear relationship with an error of  $\pm 0.01$  (see Fig. 3(c)), described by:

$$L_T = 0.19 + 0.29D_L \quad (6)$$

This demonstrates that the increase in the distance,  $D_L$  will lead to an increase in the total length of shear bands,  $L_T$ , indicating the decrease in the prohibitive ability, which corresponds to Equation 3, 5.

In order to compare the data conveniently, the three linear fitting curves (see Eqs. 3–6) were plotted in the same coordinate (see Fig. 3(d)). Obviously, both the prohibitive abilities,  $P_L$  and  $P_a$  decrease with the increase in the distance,  $D_L$ , and the two lines are nearly parallel to each other. This convinces us that the two prohibitive abilities strongly depend on the distance,  $D_L$  and accordingly, both of them are suitable parameters to weight the prohibitive effect of the limiting boundary on the propagation of shear bands in metallic glass. From the analysis above, it is easy to get the relationship between the two prohibitive abilities,  $P_L$  and  $P_a$ :

$$P_L = 0.94P_a - 0.22 \quad (7)$$

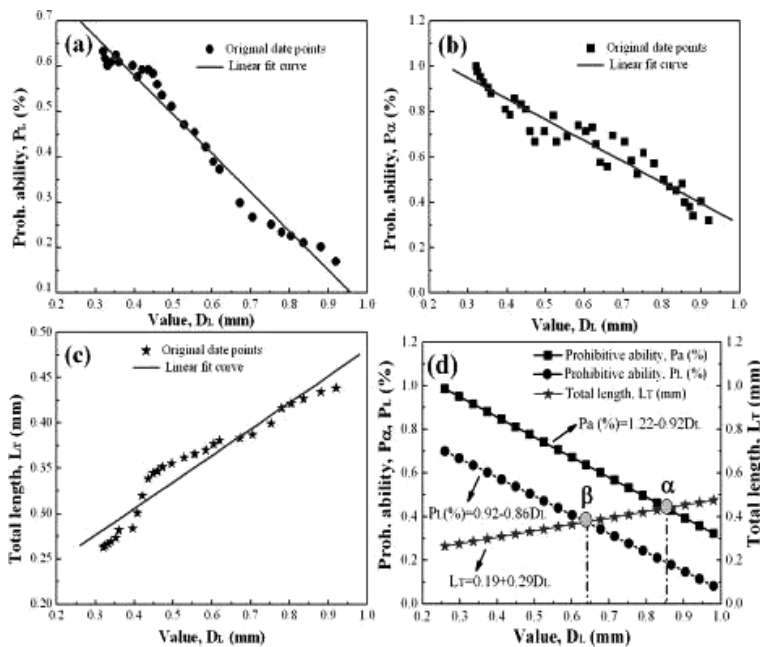


Fig. 3. Original data points and linear fitting curves for the different parameters change with the distance,  $D_L$ . (a) Prohibitive ability,  $P_L$  (%); (b) Prohibitive ability,  $P_a$  (%); (c) total length of shear bands,  $L_T$ ; and (d) three linear fitting curves with their algebraic equations.

Besides, since the total length of shear bands,  $L_T$  rises with the increase in the distance  $D_L$ , there must be the crossing points,  $\alpha$  and  $\beta$ , shown in Figure 3(d). Those are the most suitable distance,  $D_L$ , according to the rule of the prohibitive abilities,  $P_a$  and  $P_L$  respectively, to ensure both a high restraining effect and a large distance of the limiting boundary.

According to the stress distribution under the small punch test, there must be a circumferential tensile normal stress,  $\sigma_C$ , exerting on the specimen

(see Fig. 4(a)).  $\sigma_C$  can be resolved into a shear stress and a normal stress on any stress plane (see Fig. 4(c)). With the increase in loading, the maximum shear stress rises to the critical shear strength of metallic glass alloy, shear bands will initiate and then propagate along the radial direction in terms of the Tresca criterion. At the same time, there must be another tensile stress,  $\sigma_R$  that acts on the specimen, due to the fixed limiting boundary. Under the symmetric circumferential constraint, the tensile stress,  $\sigma_R$  is perpendicular to the circumferential normal stress,  $\sigma_C$ . Thus, it cannot make any effect on the propagation direction of shear bands, leading to the straight propagation of shear bands under the circumferential normal stress,  $\sigma_C$  (see Fig. 4(b)). However, under the asymmetric circumferential constraint, the tensile stress,  $\sigma_R$  is not perpendicular to the circumferential normal stress,  $\sigma_C$ . Thus, it has an important effect on the propagation direction of shear bands, leading to their deflection (see Fig. 4(b)). In detail, due to the change in the propagation direction of shear bands, the stress, triggering the formation of shear bands, will become  $\sigma_C$ , which is the resolved stress of the circumferential normal stress,  $\sigma_C$ , and it must be less than the circumferential normal stress,  $\sigma_C$ . Therefore, the shear bands will become weaker after the deflection points. Due to the continuous change in the limiting boundary, the tensile stress,  $\sigma_R$  will be altered correspondingly. Consequently, under the effect of the altered tensile stress,  $\sigma_R$ , the propagation direction of shear bands will change continually. Thus, the shear bands will interact with each other, resulting in the wriggling patterns (see Fig. 1(c,d)).

### Conclusions

In summary, although shear bands often propagate straightly in metallic glass due to its isotropic nature,<sup>[27–30]</sup> they can also display different deflection under the limiting boundary condition. The limiting boundary cannot only im-

pede the extension of shear bands, but can also restrain their growing into cracks. Recently, Zhang et al.<sup>[31]</sup> successfully enhanced the plasticity of metallic glass by controlling the residual stress on the material surface using shot-peening to induce a typical surface roughness, and also improved its strength slightly. They found that the compressive plasticity increased from an average value of 6% (maximum 7%) in as-cast samples to an average value of 11% (maximum 22%) for the shot-peened samples. This agrees well with the findings of the current study, which suggests that strengthening the surface of metallic glass should be an effective method to control the propagation and deflection of shear bands and consequently, to enhance the plasticity of metallic glass without any change in the microstructure or strength. This can contribute to toughening metallic glass materials with high strength and good plasticity by strengthening the surface.

Received: May 13, 2008

Final version: July 12, 2008

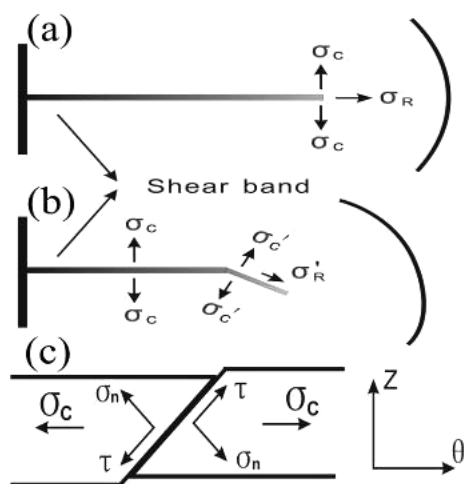


Fig. 4. Illustration for the stress distribution state, subjected to the small punch test: (a) the stress distribution state with the symmetrical limiting boundary; (b) the stress distribution state with the asymmetrical limiting boundary; (c) the resolved stress of  $\sigma_C$ : shear stress,  $\sigma_n$ , and a normal stress,  $\tau$  on any stress plane.

- [1] A. S. Argon, *Acta Metall.* **1979**, 27, 47.
- [2] L. A. Davis, *J. Mater. Sci.* **1975**, 10, 230.
- [3] L. A. Davis, S. Kavesh, *J. Mater. Sci.* **1975**, 10, 453.
- [4] P. E. Donovan, W. M. Stobbs, *Acta Mater.* **1981**, 29, 1419.
- [5] Z. F. Zhang, J. Eckert, L. Schultz, *Acta Mater.* **2003**, 51, 1167.
- [6] Y. H. Liu, G. W. Ru, J. Wang, D. Q. Zhao, M. X. Pan, W. H. Wang, *Sci.* **2007**, 315, 1385.
- [7] C. A. Schuh, T. C. Hufnagel, U. Ramamurty, *Acta Mater.* **2007**, 55, 2067.
- [8] D. B. Miracle, *Nat. Mater.* **2004**, 3, 697.
- [9] Z. F. Zhang, J. Eckert, *Phys. Rev. Lett.* **2005**, 94, 094301.
- [10] Z. F. Zhang, G. He, J. Eckert, L. Schultz, *Phys. Rev. Lett.* **2003**, 91, 045505.
- [11] J. Eckert, J. Das, S. Pauly, C. Duhamel, *J. Mater. Res.* **2007**, 22, 285.
- [12] F. Szuets, C. P. Kim, W. L. Johnson, *Acta Mater.* **2001**, 49, 1507.
- [13] C. C. Hays, C. P. Kim, W. L. Johnson, *Phys. Rev. Lett.* **2000**, 84, 2901.
- [14] Z. Bian, H. Kato, C. L. Qin, W. Zhang, A. Inoue, *Acta Mater.* **2005**, 53, 2037.
- [15] J. Eckert, U. Kühn, N. Mattern, A. R. Leonhard, M. Heilmair, *Scr. Mater.* **2001**, 44, 1587.
- [16] F. F. Wu, Z. F. Zhang, S. X. Mao, *J. Mater. Res.* **2007**, 22, 501.
- [17] Z. F. Zhang, H. Zhang, X. F. Pan, J. Das, J. Eckert, *Philos. Mag. Lett.* **2005**, 85, 513.
- [18] J. J. Kim, Y. Choi, S. Suresh, A. S. Argon, *Sci.* **2002**, 295, 654.
- [19] U. Ramamurty, S. Jana, Y. Kawamura, K. Chattopadhyay, *Acta Mater.* **2005**, 53, 705.

- [20] J. S. Park, H. K. Lim, J. H. Kim, J. M. Park, W. T. Kim, D. H. Kim, *J. Mater. Sci.* **2005**, *40*, 1937.
- [21] G. Ravichran, A. Molinari, *Acta Mater.* **2005**, *53*, 4087.
- [22] J. T. Fan, Z. F. Zhang, F. Jiang, J. Sun, S. X. Mao, *Mater. Sci. Eng. A* **2008**, *487*, 144.
- [23] Z. F. Zhang, J. Eckert, L. Schultz, *Metall. Mater. Trans.* **2004**, *35A*, 3489.
- [24] H. Chen Y. He, G. J. Shiflet, S. J. Poon, *Nature* **1994**, *367*, 541.
- [25] H. Bei, S. Xie, E. P. George, *Phys. Rev. Lett.* **2006**, *96*, 105503.
- [26] J. T. Fan, F. F. Wu, Z. F. Zhang, F. Jiang, J. Sun, S. X. Mao, *J. Non-Cryst. Solids* **2007**, *353*, 4707.
- [27] H. J. Leamy, H. S. Chen, T. T. Wang, *Metall. Trans.* **1972**, *3*, 699.
- [28] S. Henderson, J. V. Wood, G. W. Weidmann, *J. Mater. Sci. Lett.* **1983**, *2*, 375.
- [29] V. Ocelik, V. Z. Bengus, P. Diko, O. Hudak, *J. Mater. Sci. Lett.* **1987**, *6*, 1333.
- [30] T. Mukai, T. G. Nieh, Y. Kawamura, A. Inoue, K. Higashi, *Intermetall.* **2002**, *10*, 1071.
- [31] Y. Zhang, W. H. Wang, A. L. Greer, *Nat. Mater.* **2006**, *5*, 857.
-